Cancer Cell
Article

Cyclin D1 Kinase Activity Is Required for the Self-Renewal of Mammary Stem and Progenitor Cells that Are Targets of *MMTV-ErbB2* Tumorigenesis

Rinath Jeselsohn,[1,3] Nelson E. Brown,[1,3] Lisa Arendt,[1,2] Ina Klebba,[1,2] Miaofen G. Hu,[1] Charlotte Kuperwasser,[1,2,*] and Philip W. Hinds[1,*]
[1]Molecular Oncology Research Institute, Tufts Medical Center, Boston, MA 02111, USA
[2]Department of Anatomy and Cellular Biology, Tufts University School of Medicine, Boston, MA 02111, USA
[3]These authors contributed equally to this work
*Correspondence: charlotte.kuperwasser@tufts.edu (C.K.), phinds@tuftsmedicalcenter.org (P.W.H.)
DOI 10.1016/j.ccr.2009.11.024

SUMMARY

Transplantation studies have demonstrated the existence of mammary progenitor cells with the ability to self-renew and regenerate a functional mammary gland. Although these progenitors are the likely targets for oncogenic transformation, correlating progenitor populations with certain oncogenic stimuli has been difficult. Cyclin D1 is required for lobuloalveolar development during pregnancy and lactation as well as *MMTV-ErbB2*- but not *MMTV-Wnt1*-mediated tumorigenesis. Using a kinase-deficient cyclin D1 mouse, we identified two functional mammary progenitor cell populations, one of which is the target of MMTV-ErbB2. Moreover, cyclin D1 activity is required for the self-renewal and differentiation of mammary progenitors because its abrogation leads to a failure to maintain the mammary epithelial regenerative potential and also results in defects in luminal lineage differentiation.

INTRODUCTION

Breast cancer is a heterogeneous disease. Using gene expression profiling analysis, human breast cancers and mouse mammary tumor models have been broadly classified into either luminal-like or basal-like cancers (Perou et al., 2000). For example, the *MMTV-Wnt1* tumor model has been shown to classify with human basal-like breast cancers, a fact very much in keeping with the observed association of Wnt signaling in human basal-like mammary tumors (DiMeo et al., 2009; Herschkowitz et al., 2007), whereas the *MMTV-ErbB2* tumor model has been shown to classify with human luminal-type breast cancers (Herschkowitz et al., 2007). Although it is presumed that these different tumor subtypes originate from different epithelial targets, the identity of these target cells is unclear.

The mammary gland is composed of a heterogeneous population of cells ranging from terminally differentiated cells with limited proliferative potential to multipotent stem and progenitor cells with extensive proliferative, differentiative, and self-renewal capacities. Two main epithelial cell types are found in the virgin mammary tissue: luminal cells that line the lumens and express hormone receptors, and myoepithelial cells that are localized at the interface between luminal cells and the basement membrane and have specialized contractile functions. A third secretory or alveolar cell type arises during pregnancy within the terminal ductal lobular units but undergoes programmed cell death following the cessation of lactation.

An important and underappreciated feature of mammary tissues is the fact that they are composed of ducts and lobules, which are anatomically distinct structures with fundamentally different functions. Ducts are bifurcated linear structures that direct the flow of milk out of the gland whereas lobules are lateral side branching structures terminating in acinar pouchings that become alveoli during pregnancy. Consistent with this anatomical organization is the existence of multipotent progenitor cells that can be distinguished by their ability to produce lobule-limited, ductal-limited, or complete mammary outgrowths following transplantation (Kordon and Smith, 1998). All three

SIGNIFICANCE

The cellular origins of breast-cancer-initiating cells have remained obscure. In addition, the heterogeneity of breast cancers into basal and luminal types based on protein and gene expression patterns suggests that different subtypes of breast cancers might arise from different target populations of breast epithelial cells. Identification of distinct stem or progenitor cell populations with different hormonal sensitivities and requirements for cyclin D1 activity is appealing because it implies that the cellular origins of certain types of breast cancer may have a similar specificity. These specific requirements among tumor subtypes may offer therapeutic targets in human breast tumors.

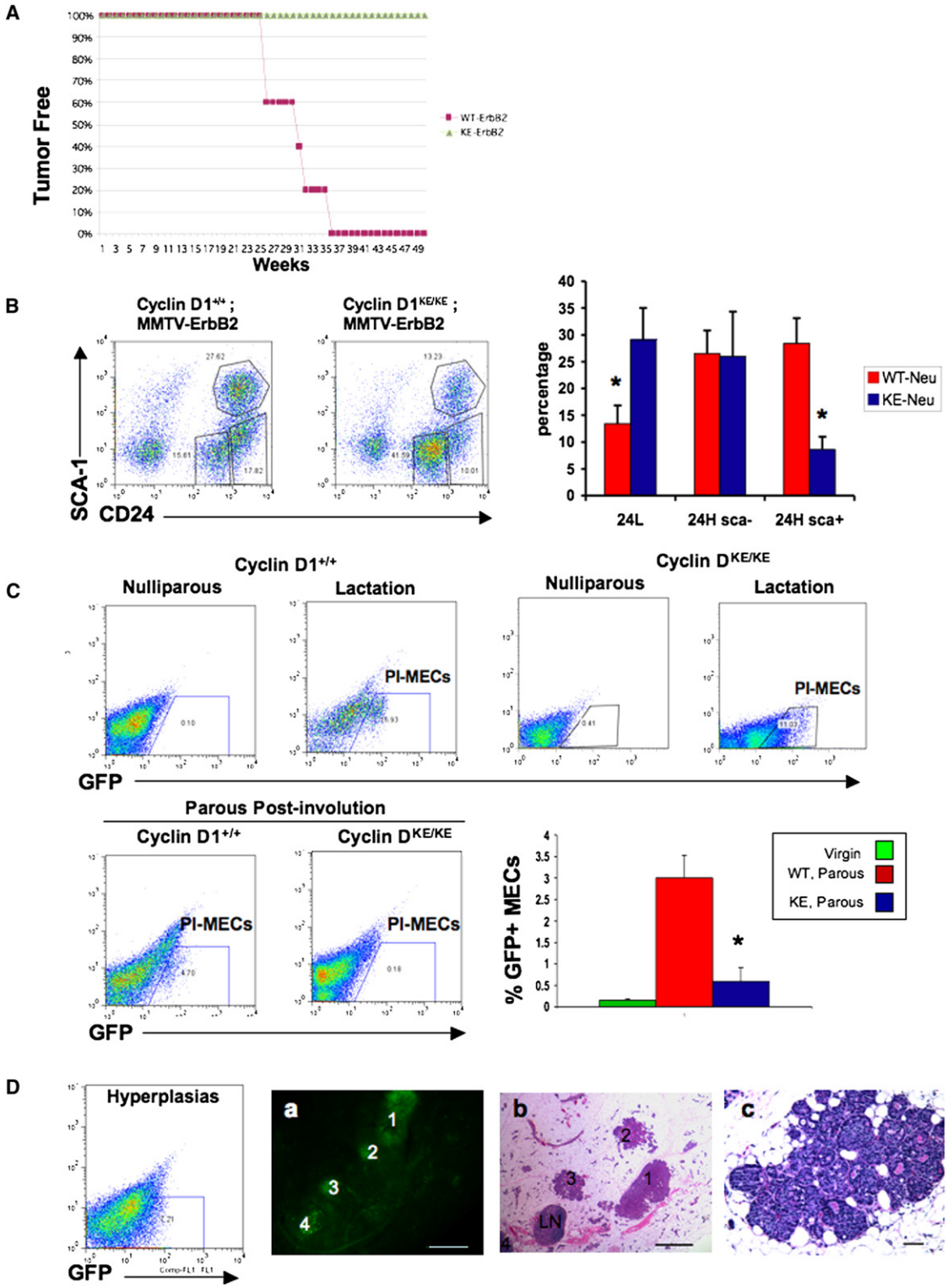

Figure 1. PI-MECs Are Reduced in Cyclin D1$^{KE/KE}$ Mice and Are the Targets of *MMTV-ErbB2*-Mediated Transformation

(A) Tumor-free curve of multiparous (three rounds of pregnancy and involution) cyclin D1$^{+/+}$/MMTV-ErbB2 and cyclin D1$^{KE/KE}$/*MMTV-ErbB2* females.

(B) Flow cytometry analysis for CD24 and Sca surface markers showing a decrease in the CD24^{+}Sca1^{+} population (24H, Sca+) in cyclin D1$^{KE/KE}$/*MMTV-ErbB2* MECs compared with cyclin D1$^{+/+}$/*MMTV-ErbB2* littermates. Error bars indicate mean and standard deviation (± SD); *p < 0.001.

(C) As shown in the upper panels: Flow cytometry analysis for the detection of GFP-positive cells in virgin and lactating cyclin D1$^{+/+}$/*MMTV-ErbB2/Wap-Cre/Rosa-GFP* mammary glands (cyclin D1$^{+/+}$: nulliparous, lactation) as well as virgin and lactating cyclin D1$^{KE/KE}$ /*MMTV-ErbB2/Wap-Cre/Rosa-GFP* (cyclin

cell types are thought to arise from a common precursor, but the precise cell types that generate ductal- or lobule-limited outgrowths have not been identified.

Several reports have described the identification of multipotent progenitor cells that exhibit self-renewal properties and can contribute to ductal, lobular, and alveolar morphogenesis (Booth et al., 2007). One type of stem/progenitor cell can be identified on the basis of a $CD24^{Med}CD29^{Hi}$ or $CD24^{+}CD49f^{Hi}$ cell surface phenotype (Shackleton et al., 2006; Stingl et al., 2006). However, a second type of progenitor cell has been reported that is capable of establishing a fully functional mammary gland upon transplantation at limiting dilution, and is able to generate all the diverse epithelial lineages present in the murine mammary tissue (Boulanger et al., 2005; Henry et al., 2004; Smith and Medina, 2008; Wagner et al., 2002). These progenitor cells, termed parity-identified mammary epithelial cells (PI-MECs), are present in both nulliparous and parous glands, and can also give rise to lobule-limited structures (Smith and Medina, 2008). At present, the link between PI-MEC progenitor cells and $CD24^{Med}CD29^{Hi}$ or $CD24^{+}CD49f^{Hi}$ populations is unclear. In addition, it has been assumed that mammary stem/progenitor cells are the targets for oncogenic transformation, but identifying which progenitor population is the target for which oncogenic stimulus has been difficult.

Cyclin D1 is a critical component of the cell cycle that is required for mammary gland development. Cyclin D1-knockout mice fail to generate lobuloalveoli during pregnancy and cannot lactate (Fantl et al., 1995; Sicinski et al., 1995). Interestingly, cyclin D1 knockout mice are resistant to *MMTV-ErbB2*-mediated tumorigenesis, a fact very much in keeping with the observed overexpression of cyclin D1 in the majority of human luminal mammary tumors (Gauthier et al., 2007; Yu et al., 2001). In contrast, cyclin D1 knockout mice are still susceptible to *MMTV-Wnt1*-mediated oncogenesis, suggesting the possibility that these tumors originate from different epithelial targets that exhibit different sensitivities to cyclin D1 expression.

In order to dissect the roles of cyclin D1-associated kinase activity during mammary gland development and *MMTV-ErbB2*-induced tumorigenesis, we have generated the point mutant cyclin D1 (*K112E*) knockin mouse. The cyclin D1-K112E protein can still bind to cyclin-dependent kinases 4 and 6 (Cdk4/6) but the resulting complexes are enzymatically inactive (Baker et al., 2005; Hinds et al., 1994). We have previously shown that cyclin $D1^{KE/KE}$ female mice displayed apparently developed lobuloalveoli following pregnancy, yet they remained protected against the development of *MMTV-ErbB2*-driven mammary tumors (Landis et al., 2006). In the current study, we sought to determine the cellular mechanisms by which the absence of cyclin D1-associated kinase activity does not seem to affect development but can block the formation of *ErbB2*-driven mammary tumors.

RESULTS

PI-MEC Progenitor Cells Are the Targets of *MMTV-ErbB2*-Mediated Tumorigenesis and Cannot Be Maintained in Cyclin $D1^{KE/KE}$ Mutant Mice

We have previously reported that nulliparous mice deficient in cyclin D1 kinase activity failed to develop mammary tumors on an *MMTV-ErbB2* background despite exhibiting normal lobuloalveolar development after a single round of pregnancy and lactation (Landis et al., 2006). However, it has been well established that the development of *MMTV-ErbB2*-driven mammary tumors can be accelerated following repeated cycles of pregnancy (Henry et al., 2004). Therefore, we first sought to determine whether multiple pregnancies in cyclin $D1^{KE/KE}$ mice might overcome their tumor resistance. We found that after three rounds of consecutive breeding cycles, cyclin $D1^{KE/KE}$/MMTV-ErbB2 mice remained resistant to the development of mammary tumors (Figure 1A). In contrast, cyclin $D1^{+/+}$/*MMTV-ErbB2* mice exhibited accelerated mammary tumors as expected.

We next wanted to determine whether the inability of cyclin $D1^{KE/KE}$ mice to develop *MMTV-ErbB2*-driven tumors was due to a reduction in the number of the cellular targets for transformation. Recently, the cellular targets of *MMTV-ErbB2*-induced tumorigenesis have been suggested to reside within PI-MECs in parous animals (Boulanger et al., 2005; Henry et al., 2004; Smith and Medina, 2008; Wagner et al., 2002) as well as within a population of cells exhibiting a $CD24^{+}Sca1^{+}$ phenotype (Li et al., 2007; Liu et al., 2007). Therefore, we examined the number of $CD24^{+}Sca1^{+}$ cells as well as PI-MECs in cyclin $D1^{KE/KE}$ mice. FACS analysis performed on single-cell suspensions of mammary epithelium revealed a ~3-fold reduction in the number of $CD24^{+}Sca1^{+}$ progenitor cells and a ~2-fold increase in $CD24^{Low}$ cells present in mammary glands of cyclin $D1^{KE/KE}$/*MMTV-ErbB2* mice (Figure 1B). However, the fact that $CD24^{+}Sca1^{+}$ cells were still present in cyclin $D1^{KE/KE}$ mice suggested that this population might not be the cellular target for transformation.

We next assessed the number of PI-MECs in cyclin $D1^{KE/KE}$ mammary glands (Smith and Medina, 2008). Accordingly, we generated cyclin $D1^{KE/KE}$/*MMTV-ErbB2/WAP-cre/Rosa-GFP* mice in which the green fluorescent protein (GFP) is expressed following pregnancy-induced Cre-mediated recombination. As expected, the generation of GFP^{+} cells was confirmed during lactation in both cyclin $D1^{+/+}$ and cyclin $D1^{KE/KE}$ mice (Figure 1C, upper panels). Six weeks after postlactational involution, we continued to detect a population of GFP^{+} cells in parous mammary glands of cyclin $D1^{+/+}$/*MMTV-ErbB2/WAP-cre/Rosa-GFP* mice

$D1^{KE/KE}$: nulliparous, lactation). As shown in the lower panels and graph: Flow cytometry analysis showing GFP-positive cells (PI-MECs) derived from cyclin $D1^{+/+}$/*MMTV-ErbB2/Wap-Cre/Rosa-GFP* (cyclin $D1^{+/+}$) and cyclin $D1^{KE/KE}$/*MMTV-ErbB2/Wap-Cre/Rosa-GFP* (cyclin $D1^{KE/KE}$) mammary glands 6 weeks postlactational involution. Error bars indicate mean ± SD; *$p < 0.001$.

(D) The expansion of the GFP-positive cells was detected by flow cytometry analysis performed on MECs derived from a parous nonpregnant cyclin $D1^{+/+}$/*MMTV-ErbB2/Wap-Cre/Rosa-GFP* mammary gland with early hyperplastic lesions (hyperplasias). (a) shows a freshly isolated mammary gland from a parous nonpregnant cyclin $D1^{+/+}$/*MMTV-ErbB2/Wap-Cre/Rosa-GFP* mouse revealing GFP positive lesions (numbered 1 to 4) under fluorescence microscopy. The scale bar represents 100 μm. As shown in (b), hematoxylin and eosin (H&E)-stained section from the same mammary gland in (a) showing that GFP-positive lesions represent early hyperplastic lesions. The lymph node (LN) is GFP negative. The scale bar represents 100 μm. (c) shows a higher magnification of a hyperplastic lesion. The scale bar represents 50 μm.

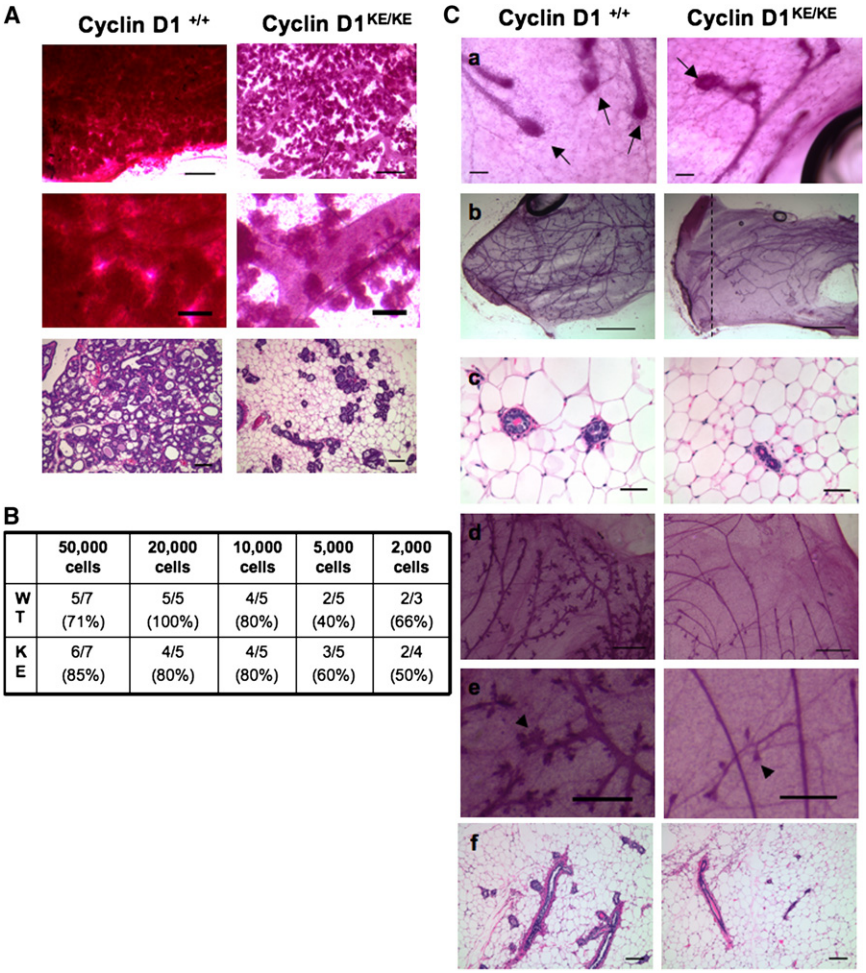

B

	50,000 cells	20,000 cells	10,000 cells	5,000 cells	2,000 cells
WT	5/7 (71%)	5/5 (100%)	4/5 (80%)	2/5 (40%)	2/3 (66%)
KE	6/7 (85%)	4/5 (80%)	4/5 (80%)	3/5 (60%)	2/4 (50%)

Figure 2. Cyclin D1 Kinase Activity Is Required for the Maintenance and Activity of Progenitor Cells in the Mammary Gland

(A) Mammary glands obtained from multiparous (three rounds of pregnancy and involution) cyclin $D1^{+/+}$ and cyclin $D1^{KE/KE}$ mice were morphologically analyzed 1 day postpartum. Whole mounts and H&E-stained sections are shown. Notice the failure to undergo normal lobuloalveolar expansion observed in cyclin $D1^{KE/KE}$ mammary tissue. Middle panels represent a higher magnification of top panels. Scale bars represent 100 μm on the top; middle, 25 μm in the middle, and 100 μm on the bottom.

(B) Summary of dilutional transplantation experiments showing that cyclin $D1^{+/+}$ and cyclin $D1^{KE/KE}$ MECs have similar engrafting capacity. The number of successful transplants per total injections is indicated.

(C) Ductal outgrowths derived from transplantation of cyclin $D1^{KE/KE}$ MECs have normal terminal end buds (a). The scale bar represents 100 μm. Arrows indicate terminal end buds. As shown in (b), cyclin $D1^{KE/KE}$ ductal outgrowths fail to reach the end of the fat pad. The scale bar represents 200 μm. (c) shows decrease in the size of the ducts derived from cyclin $D1^{KE/KE}$ MECs transplants as seen in H&E staining. The scale bar represents 40 μm. (d)–(f) show profound reduction in the side branching and lobule outgrowths derived from cyclin $D1^{KE/KE}$ MECs. Whole-mount analysis (d) and H&E staining (f) are shown. Middle panels represent a higher magnification of top panels. Scale bars represent 100 μm in (d), 50 μm in (e), and 100 μm in (f). See also Table S1 and Figure S1.

consistent with the labeling of PI-MECs. In contrast, parous cyclin $D1^{KE/KE}$/*MMTV-ErbB2/WAP-cre/Rosa-GFP* mammary tissues retained very few GFP^+ cells (Figure 1C, lower panels).

The near absence of PI-MECs in cyclin $D1^{KE/KE}$/*MMTV-ErbB2* mice suggested that this population might contain the cell of origin for tumorigenesis in this model. Indeed, premalignant lesions originated in parous cyclin $D1^{+/+}$/*MMTV-ErbB2/WAP-cre/Rosa-GFP* mice were invariably GFP^+, confirming that they were derived from PI-MECs (Figure 1D) (Henry et al., 2004). Collectively, these findings indicate that cyclin $D1^{KE/KE}$ mice are resistant to *MMTV-ErbB2*-induced tumorigenesis due to a lack of cellular targets of transformation, namely PI-MECs.

Cyclin D1 Activity Is Required for Mammary Progenitor Cell Self-Renewal and Activity

The fact that virtually no PI-MECs were detectable in parous cyclin $D1^{KE/KE}$ mammary glands suggested a failure of this population to self-renew and, therefore, to be maintained following pregnancy. Consequently, we speculated that these mice might exhibit defects in the ability to form lobuloalveoli following successive cycles of pregnancy-induced proliferation and differentiation. Indeed, mammary tissues from cyclin $D1^{KE/KE}$ mice showed a pronounced failure to undergo full lobuloalveolar differentiation after a third pregnancy (Figure 2A). This observation combined with the inability to maintain PI-MECs indicates that cyclin D1-associated kinase activity is necessary for the maintenance of progenitor cells.

To determine the extent to which other progenitor cell activities might also be compromised in the absence of cyclin D1 kinase activity, we examined the regenerative capacity of MECs isolated from mutant and wild-type mice following transplantation into cleared fat pads. Bipotent stem cells give rise to two types of progenitor cells that mediate regenerative activities: ductal progenitors that give rise to cap cells and drive ductal elongation through the terminal end bud structure, and the lobule progenitors that produce the progeny for the side branches and lobular-alveolar development (Smith and Medina, 2008). Single-cell suspensions of cyclin $D1^{KE/KE}$ or cyclin $D1^{+/+}$ MECs were transplanted into contralateral cleared fat pads in a dilution series ranging from 50,000 to 2,000 cells. Both cyclin $D1^{+/+}$ and cyclin $D1^{KE/KE}$ MECs exhibited comparable engraftment rates at limiting dilutions and formed terminal end buds at the growing tips of the penetrating ducts 5 weeks after transplantation (Figures 2B and 2C, a). However, nearly 75% of all the outgrowths derived from cyclin $D1^{KE/KE}$ MECs failed to fill the entire fat pads while this only occurred in 35% of the transplants from cyclin $D1^{+/+}$ cells (Figures 2C, b; see also Table S1 available

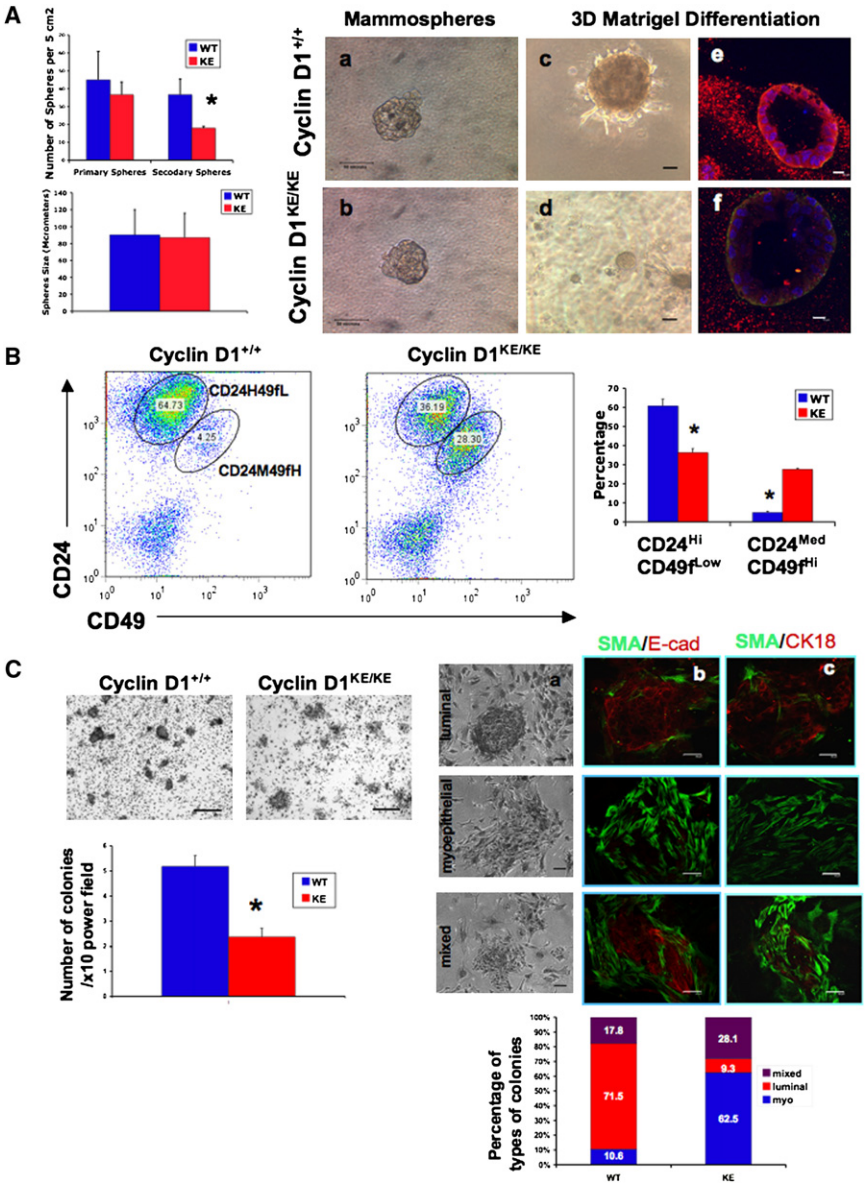

Figure 3. Lack of Cyclin D1 Kinase Activity Leads to Decreased Self-Renewal of Mammary Progenitors and a Reduction in the CD24^{Hi}CD49f^{Low} Population

(A) The left panels show sphere formation assays for cyclin D1$^{+/+}$ and cyclin D1$^{KE/KE}$ MECs plated in low-attachment plates and serum-free conditions (see Experimental Procedures). Quantification of the number of primary and secondary spheres per 5 cm^2 and the size of secondary mammospheres (in μm) is shown. There was no significant difference in the number of primary spheres formed by cyclin D1$^{+/+}$ and cyclin D1$^{KE/KE}$ MECs ($p = 0.236$). The number of secondary spheres, however, was significantly reduced in the context of KE mutation ($p < 0.05$). The size of secondary spheres was similar between genotypes. Error bars indicate mean ± SD; *$p < 0.05$. As shown in the right panels, secondary spheres derived from cyclin D1$^{+/+}$ and cyclin D1$^{KE/KE}$ MECs (a and b) were dissociated on day 21 and embedded in Matrigel (c and d). The resulting acinar structures were stained for DAPI (blue), smooth muscle actin (green) and E-cadherin (red) and analyzed by confocal microscopy (e and f). Scale bars represent 50 μm in (a)–(d) and 10 μm in (e) and (f).

(B) Flow cytometry analysis showing the distribution of Lin(−) MECs for the expression of the surface markers CD24 and CD49f. Notice the decrease in the CD24^{Hi}CD49f^{Low} and the increase in the CD24^{Med}CD49f^{Hi} cell fractions in cyclin D1$^{KE/KE}$ MECs compared with cyclin D1$^{+/+}$ MECs. Error bars indicate mean ± SD; *$p < 0.01$.

(C) As shown in the left panels: Crystal violet staining of epithelial colonies formed on a feeder layer of growth-arrested fibroblasts (see Experimental Procedures). Quantification of the number of colonies per 10x field is shown. Notice the reduction in the number of colonies generated by cyclin D1$^{KE/KE}$ MECs. Error bars indicate mean ± SD; *$p < 0.001$. As shown in the right panels: Three distinct types of colonies (luminal, myoepithelial, and mixed) were identified based on both morphology (a) and immunostaining (b and c). A quantification of the proportions of the different types of colonies derived from cyclin D1$^{+/+}$ and cyclin D1$^{KE/KE}$ MECs is shown. SMA, smooth muscle actin; E-cad, E-cadherin; CK18, cytokeratin 18. Scale bars represent 20 μm in (a) and 50 μm in (b) and (c). See also Figure S2.

online). In addition, there was a reduction in the overall number of ducts as well as a decrease in ductal size of mammary trees derived from cyclin D1$^{KE/KE}$ MECs (Figure 2C, b and c). Importantly, the ductal system derived from cyclin D1$^{KE/KE}$ MECs was nearly devoid of all side branching and lobules (Figure 2C, d–f, and Figure S1). This observation was independent of the number of cells transplanted or the estrus status of the recipient mice at the time of sacrifice (see Experimental Procedures). This finding indicates that mammary progenitor cell self-renewal is compromised in the absence of cyclin D1-associated kinase activity.

To further assess the defect in self-renewal activity, we examined the ability of cyclin D1$^{KE/KE}$ and cyclin D1$^{+/+}$ MECs to form spheres under nonadherent and serum free conditions (Dontu et al., 2003). We found that cyclin D1$^{+/+}$ and cyclin D1$^{KE/KE}$ MECs formed similar numbers of primary spheres (45 ± 15.9 versus 36.7 ± 8.7 for wild-type and KE, respectively, $p = 0.236$; Figure 3A, left panels). However, secondary sphere formation was reduced ~2-fold in cyclin D1$^{KE/KE}$ MECs compared with cyclin D1$^{+/+}$ MECs (18.0 ± 1.0 versus 36.7 ± 7.1 for KE and wild-type cells, respectively, $p = 0.0212$; Figure 3A, left panels) suggesting that the self-renewal capacity of progenitors was impaired in the absence of cyclin D1-associated kinase activity. We failed to observe any differences in the size of spheres between genotypes (Figure 3A left panels, and Figure 3A, a and b). Taken together, these data indicate that cyclin D1 activity is necessary for the regeneration of mammary tissues and the self-renewal of mammary progenitor cells.

We also examined colony formation of sphere-derived cells in Matrigel. Colonies generated from mutant spheres grew as spherical acinar structures that were smaller in size compared with those derived from cyclin $D1^{+/+}$ spheres (Figure 3A, c and d). In addition, confocal immunofluorescence microscopy analysis revealed that cyclin $D1^{KE/KE}$ acini were composed of an outer layer of SMA+ myoepithelial cells and an inner layer of luminal cells that failed to express E-cadherin (Figure 3A, e and f). This suggested that colony forming progenitor cells from cyclin $D1^{KE/KE}$ mammary glands lack full bipotent activity compared with those derived from cyclin $D1^{+/+}$ mammary glands (see below). Taken together, these data indicate that cyclin D1 activity is necessary for regeneration of mammary tissues and for the self-renewal and differentiation of mammary progenitor cells.

Mammary Tissues Lacking Cyclin D1 Activity Have Reduced Bipotent $CD24^{Hi}CD49f^{Low}$ Cells

Because PI-MEC progenitors cannot be maintained in mammary glands of mice lacking cyclin D1 kinase activity, we reasoned that we could identify this population of cells by fluorescence-activated cell sorting (FACS) because it should be absent or greatly reduced in virgin cyclin $D1^{KE/KE}$ mice. Stem/progenitor cells with regenerative activity following transplantation into cleared fat pads can be enriched in either $CD24^{Med}CD29^{Hi}$ or $CD24^{Med}CD49f^{Hi}$ populations (Matulka et al., 2007; Shackleton et al., 2006; Stingl et al., 2006). Therefore, we first examined the distribution of CD24 and CD29 markers in cyclin $D1^{KE/KE}$ and cyclin $D1^{+/+}$ MEC preparations that were gated for CD45(-) cells. We found no significant difference in the number of $CD24^{Med}CD29^{Hi}$ cells in cyclin $D1^{KE/KE}$ mammary glands compared with cyclin $D1^{+/+}$ tissues, suggesting that this population of progenitors was not affected by cyclin D1 activity (Figure S2A).

We next analyzed Lin(−) MECs from cyclin $D1^{KE/KE}$ mice using the cell surface markers CD24 and CD49f. Consistent with previous reports (Stingl et al., 2006), we identified two populations of cells in cyclin $D1^{+/+}$ as well as cyclin $D1^{KE/KE}$ mammary glands (Figure 3B). Noncommitted progenitor cells are reported to reside within both $CD24^{Med}CD49f^{Hi}$ and $CD24^{Hi}CD49f^{Low}$ populations. $CD24^{Med}CD49f^{Hi}$ cells enrich for mammary reconstitution units that can regenerate an entire mammary tissue following transplantation, whereas $CD24^{Hi}CD49f^{Low}$ cells enrich for colony-forming cells that can form heterogeneous colonies when plated in vitro (Stingl et al., 2006). Despite the reduced regenerative potential of cyclin $D1^{KE/KE}$ MECs, we found that mammary glands lacking cyclin D1 kinase activity contained increased numbers of $CD24^{Med}CD49f^{Hi}$ cells but a significant decrease in $CD24^{Hi}CD49f^{Low}$ cells (Figure 3B).

Because cells with the ability to form adherent colonies in vitro are enriched within the $CD24^{Hi}CD49f^{Low}$ fraction (Stingl et al., 2001), and this population was reduced in cyclin $D1^{KE/KE}$ mammary tissues, we reasoned that the colony-forming capacity of cyclin $D1^{KE/KE}$ MECs should be impaired. Indeed, we found that cyclin $D1^{KE/KE}$ MECs displayed decreased colony-forming potential compared with cyclin $D1^{+/+}$ MECs (Figure 3C, left panels). When primary MECs are assayed in this way, they form three distinct luminal, myoepithelial, and mixed colonies, derived from luminal, myoepithelial, and bipotent progenitors, respectively (Stingl et al., 2001). Luminal colonies consist of tightly arranged cuboidal cells, whereas pure myoepithelial colonies have dispersed, teardrop-shaped cells. Mixed colonies are composed of a central core of tightly arranged cells surrounded by more dispersed cells. We observed that both cyclin $D1^{KE/KE}$ and cyclin $D1^{+/+}$ MECs were able to form all three types of colonies as confirmed by staining for alpha-smooth muscle actin (SMA), E-cadherin, and cytokeratin 18 (CK18) (Figure 3C, a-c). However, cyclin $D1^{KE/KE}$ MECs formed fewer luminal colonies as well as greater numbers of myoepithelial colonies compared with MECs derived from cyclin $D1^{+/+}$ mammary tissues (Figure 3C, right panels). Consistent with this shift in cell fate in $D1^{KE/KE}$ MECs, we observed that cyclin D1 was expressed almost exclusively in luminal epithelial cells, but not in myoepithelial cells in these colonies (Figure S2B). These findings suggested that colony-forming progenitor cells from cyclin $D1^{KE/KE}$ mammary glands lack full bipotent activity compared with those from cyclin $D1^{+/+}$ mammary glands.

Mammary Tissues Contain Distinct Progenitor Cell Populations

The fact that cyclin $D1^{KE/KE}$ MECs are defective in progenitor cells with the ability to self-renew yet exhibit an increase in $CD24^{Med}CD49f^{Hi}$ cells would seem conceptually inconsistent with the current mammary stem/progenitor cell model. Therefore, we first needed to exclude the possibility that $CD24^{Med}CD49f^{Hi}$ cells might require cyclin D1 activity for proper function and differentiation. Accordingly, we examined the differentiation potential of sorted $CD24^{Hi}CD49f^{Low}$ and $CD24^{Med}CD49f^{Hi}$ cells from cyclin $D1^{KE/KE}$ and cyclin $D1^{+/+}$ mammary tissues. Progenitor cells within the $CD24^{Hi}CD49f^{Low}$ population form spherical acinar structures, whereas $CD24^{Med}CD49f^{Hi}$ cells form solid, irregular-shaped colonies when embedded in Matrigel (Stingl et al., 2006). Indeed, wild-type $CD24^{Hi}CD49f^{Low}$ cells formed predominantly hollow spherical colonies, whereas $CD24^{Med}CD49f^{Hi}$ cells formed predominantly solid spheres (Figure 4A). Importantly, we found that sorted $CD24^{Hi}CD49f^{Low}$cells from cyclin $D1^{KE/KE}$ mice displayed a marked decrease in the formation of large hollow acini compared with those derived from wild-type controls while the number and size of $CD24^{Med}CD49f^{Hi}$- derived colonies was indistinguishable between genotypes (Figure 4A and data not shown). In addition, we also examined the differentiation potential of Matrigel colonies for the presence of myoepithelial markers (cytokeratin 14 and SMA) and luminal epithelial markers (cytokeratin 18 and E-cadherin). $CD24^{Med}CD49f^{Hi}$ MECs from cyclin $D1^{+/+}$ and cyclin $D1^{KE/KE}$ mammary tissues gave rise to similar numbers of colonies expressing the myoepithelial markers SMA or cytokeratin 14, or the luminal epithelial markers cytokeratin 18 or E-cadherin (Figure 4B, Figure S3A, and data not shown). However, sorted $CD24^{Hi}CD49f^{Low}$ cells from cyclin $D1^{KE/KE}$ tissues gave rise to a higher proportion of colonies containing SMA+ cells (Figure 4B) compared with sorted $CD24^{Hi}CD49f^{Low}$ cells from cyclin $D1^{+/+}$ glands, suggesting a defect in the differentiation potential of this population in the absence of cyclin D1 kinase activity. To further confirm our findings, we assessed the mRNA expression levels of *CD61*, a reported marker for luminal progenitor cells (Asselin-Labat et al., 2007), in CD24/CD49f-sorted populations. We observed a significant 2-fold decrease in *CD61* expression in $CD24^{Hi}CD49f^{Low}$

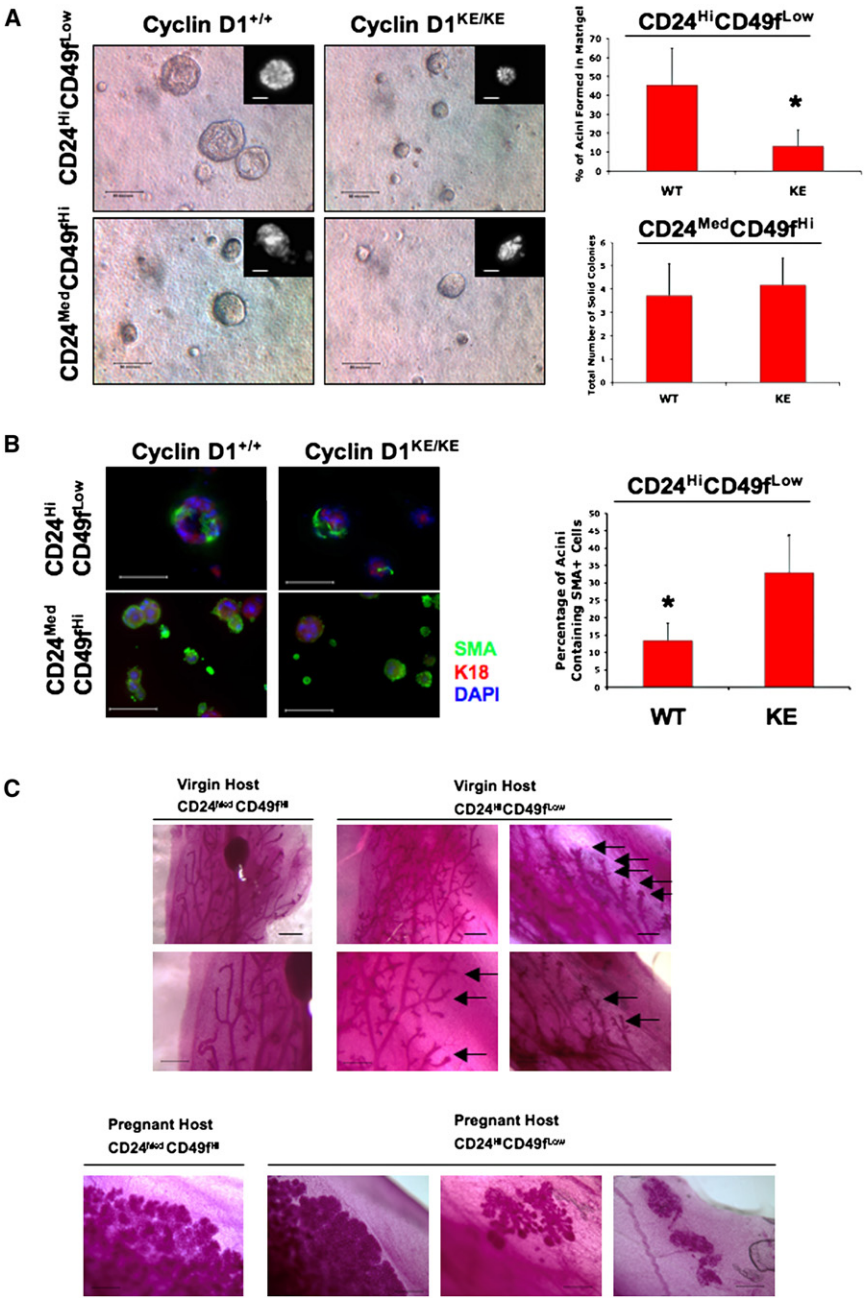

Figure 4. Mammary Tissues Lacking Cyclin D1 Kinase Activity Have Reduced Bipotent $CD24^{Hi}CD49f^{Low}$ Cells

(A) $CD24^{Hi}CD49f^{Low}$ and $CD24^{Med}CD49f^{Hi}$ populations derived from cyclin $D1^{+/+}$ and cyclin $D1^{KE/KE}$ MECs were embedded in Matrigel (Debnath et al., 2003) and the type and number of colonies formed was microscopically assessed 10 days later. As expected, $CD24^{Hi}CD49f^{Low}$ cells derived from cyclin $D1^{+/+}$ MECs gave rise to large lumen-containing structures (acini). However, the number of acini formed by $CD24^{Hi}CD49f^{Low}$ cells was dramatically reduced in the context of cyclin D1 kinase activity deficiency. No significant difference was in the number and size of solid colonies generated from $CD24^{Med}CD49f^{Hi}$ populations of either genotype. Insets show DAPI-stained representative colonies. The scale bar represents 50 μm. Error bars indicate mean ± SD; *$p < 0.01$.

(B) Colonies generated in (A) were subjected to immunofluorescence for the detection of myoepithelial (SMA) and luminal epithelial cell (K18) markers. Most acini generated from wild-type $CD24^{Hi}CD49f^{Low}$ cells were negative for SMA. However, ~12% of them showed the presence of SMA-positive cells. This proportion was increased to ~30% in colonies generated from mutant $CD24^{Hi}CD49f^{Low}$ cells. On the other hand, most structures generated from $CD24^{Med}CD49f^{Hi}$ cells were strongly positive for SMA (>90%), with ~20% of them showing strong K18 costaining. No differences in staining between genotypes were observed in this fraction of cells. SMA, smooth muscle actin; K18, keratin-18. The scale bar represents 50 μm. Error bars indicate mean ± SD; *$p < 0.001$. See also Figures S3A and S3B.

(C) The upper panels show whole mounts of outgrowths derived from sorted $CD24^{Med}CD49f^{Hi}$ and $CD24^{Hi}CD49f^{Low}$ populations purified from wild-type nulliparous mice. A total of 5×10^4 $CD24^{Med}CD49f^{Hi}$ or 5×10^4 $CD24^{Hi}CD49f^{Low}$ cells were injected into cleared fat pads of virgin Balb/c female mice. Representative ductal trees illustrate the duct-only derived growths from sorted $CD24^{Med}CD49f^{Hi}$ cells while $CD24^{Hi}CD49f^{Low}$ cells gave rise to ducts and lobules under the same conditions. Arrows: lobule side branches. The lower panels show lobular/alveolar outgrowths derived from sorted $CD24^{Med}CD49f^{Hi}$ and $CD24^{Hi}CD49f^{Low}$ cells transplanted into cleared fat pads of pregnant hosts. A total of 5×10^4 $CD24^{Med}CD49f^{Hi}$ or 5×10^4 $CD24^{Hi}CD49f^{Low}$ cells were injected into cleared fat pads of pregnant Balb/c female mice. Representative whole mounts of ductal/alveolar trees illustrating the lobular/alveolar growths derived from sorted $CD24^{Med}CD49f^{Hi}$ and $CD24^{Hi}CD49f^{Low}$ cells are shown. Note that $CD24^{Hi}CD49f^{Low}$ cells also produced lobule-only and acinar-only growths in pregnant hosts. Scale bars represent 500 μm. See also Figure S3C.

MECs derived from cyclin $D1^{KE/KE}$ mammary glands compared with the same population derived from wild-type MECs (Figure S3B). However, there was no significant difference in *CD61* expression between $CD24^{Med}CD49f^{Hi}$ fractions from cyclin $D1^{KE/KE}$ and cyclin $D1^{+/+}$ MECs (Figure S3B). Although these findings demonstrate that $CD24^{Med}CD49f^{Hi}$ as well as $CD24^{Hi}CD49f^{Low}$ populations both contain bipotent progenitor cells, only $CD24^{Hi}CD49f^{Low}$ cells exhibit defects in differentiation potential in the absence of cyclin D1 kinase activity.

Our findings suggest that a proportion of $CD24^{Hi}CD49f^{Low}$ cells contain bipotential progenitor activity, and this activity is impaired in the absence of cyclin D1 kinase activity. We therefore assessed the in vivo reconstitution activity of sorted $CD24^{Med}CD49f^{Hi}$ and $CD24^{Hi}CD49f^{Low}$ cells (5×10^4) derived from wild-type mammary glands following transplantation into cleared mammary fat pads of either nulliparous (virgin) or pregnant hosts (Figure 4C). Consistent with previous studies, we found that sorted $CD24^{Med}CD49f^{Hi}$ cells were indeed capable of

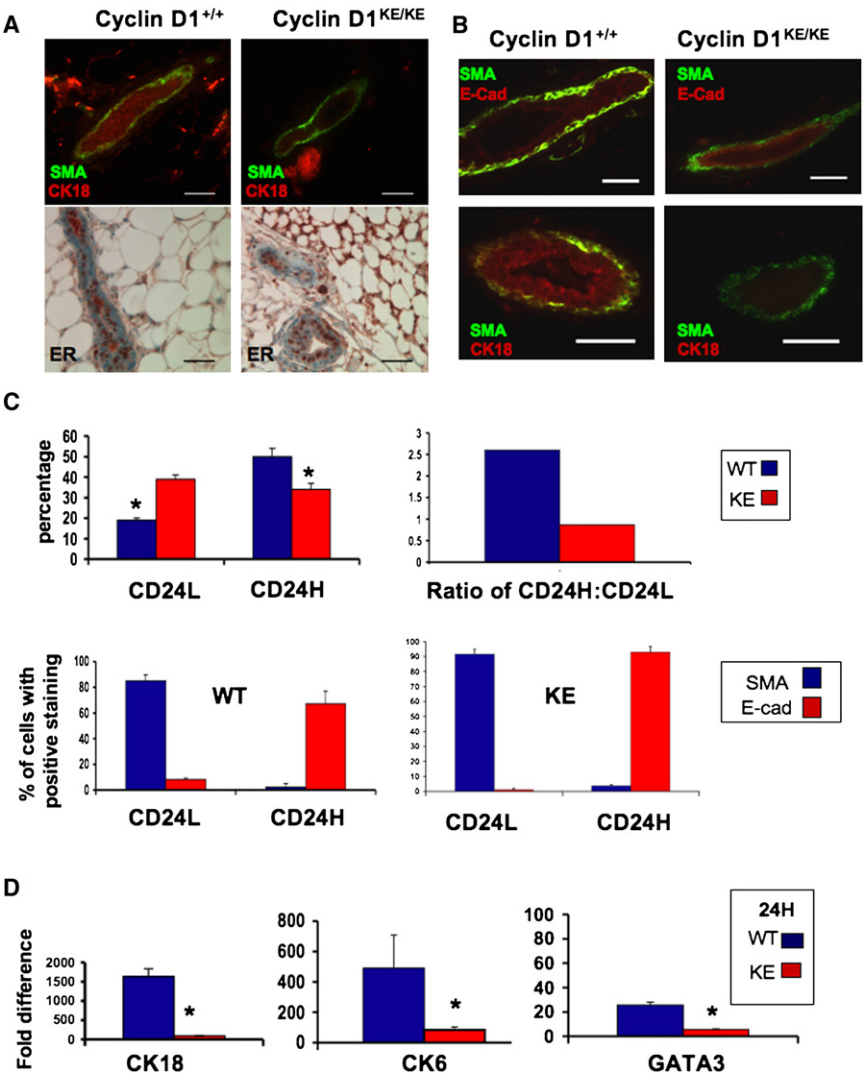

Figure 5. Defects in Luminal-Lineage Differentiation in the Absence of Cyclin D1 Kinase Activity

(A) Immunofluorescence and immunohistochemical analysis of innate mammary glands derived from cyclin D1$^{+/+}$ and cyclin D1$^{KE/KE}$ mice. Costainings for SMA (green) and CK18 (red) and stainings for estrogen receptor alpha (ER) are shown. Notice the reduced CK18 staining in cyclin D1$^{KE/KE}$ tissue compared with its cyclin D1$^{+/+}$ counterpart. No difference in ER staining was observed. SMA, smooth muscle actin; CK18, cytokeratin-18; ER, estrogen receptor. The scale bar represents 40 μm.

(B) Immunofluorescence staining of ducts derived from transplants of cyclin D1$^{+/+}$ and cyclin D1$^{KE/KE}$ MECs for the myoepithelial marker SMA (green) and luminal markers E-cadherin or CK18 (red). SMA, smooth muscle actin; CK18, cytokeratin-18; E-Cad, E-cadherin. The scale bar represents 40 μm. See also Figure S4A.

(C) As shown in the upper panels, cyclin D1$^{+/+}$ and cyclin D1$^{KE/KE}$ MECs were analyzed by flow cytometry for the expression of the surface marker CD24. There was an increase in the CD24^{Low} population (CD24L) and a reduction in the CD24^{Hi} population (CD24H) in cyclin D1$^{KE/KE}$ MECs (KE) compared with cyclin D1$^{+/+}$ MECs (WT). The CD24H: CD24L ratio for each genotype is also shown. *p < 0.05. As shown in the lower panels, CD24-sorted cells were cytospun directly on glass slides and subsequently stained by for SMA and E-cadherin. As expected, the majority of CD24^{Hi} cells (CD24H) were E-cadherin positive and SMA negative and the opposite was observed for CD24^{Low} populations (CD24L). SMA, smooth muscle actin; E-Cad, E-cadherin. Error bars indicate mean ± SD. See also Figure S4B.

(D) Gene expression analysis of CD24^{Hi} populations for CK18, CK6, and GATA3 by quantitative RT-PCR. Error bars indicate mean ± SD; *p < 0.01.

ductal and lobular/alveolar development when transplanted into cleared fat pads of pregnant hosts, indicating that cells within this population have the capacity to undergo full lobuloalveolar differentiation under pregnancy-induced conditions (Stingl et al., 2006). However, we found that the ductal trees derived from CD24^{Med}CD49f^{Hi} MECs injected into nulliparous hosts were nearly devoid of all side branching and lobule development, indicating that CD24^{Med}CD49f^{Hi} cells were unable to give rise to lobular/alveolar development in the absence of pregnancy (Figure 4C).

Moreover, we found that injection of CD24^{Hi}CD49f^{Low} cells not only generated ductal and lobular/alveolar outgrowths in pregnant hosts but also lobule-only and alveolar-only outgrowths (Figure 4C). Furthermore, we found that sorted CD24^{Hi}CD49f^{Low} cells produced ductal and lobular development with extensive side branching in nulliparous hosts, indicating that bipotent progenitor cells reside within this fraction and that these cells do not depend on the hormones of pregnancy for their differentiation potential (Figure 4C). It is worth noting that while CD24^{Med}CD49f^{Hi} and CD24^{Hi}CD49f^{Low} cells resulted in comparable engraftment rates and fat-pad filling in the nulliparous host, sorted CD24^{Med}CD49f^{Hi} cells did exhibit a slight increase in fat-pad filling in pregnant hosts, consistent with the notion that CD24^{Med}CD49f^{Hi} cells enrich for cells with greater mammary reconstituting activity in pregnant mice (Figure S3C) (Stingl et al., 2006).

Defects in Luminal-Lineage Differentiation in the Absence of Cyclin D1 Kinase Activity

The data described above demonstrate a cyclin D1-activity dependence for the formation of lobular-alveolar structures, and also indicate that the ratio of luminal and myoepithelial cells is altered in cyclin D1$^{KE/KE}$ animals. To further explore this defect in epithelial differentiation, we stained cyclin D1$^{KE/KE}$ or cyclin D1$^{+/+}$ mammary tissues for markers of luminal (K18) and myoepithelial (SMA) differentiation. We found that myoepithelial cells within the main ducts of cyclin D1$^{KE/KE}$ and cyclin D1$^{+/+}$ mammary glands expressed SMA, but luminal cells in cyclin D1$^{KE/KE}$ glands lacked a robust K18 expression compared with cyclin D1$^{+/+}$ ducts (Figure 5A). In addition, although some reports suggest that keratin-6 (K6) is a marker of mammary progenitor cells, others have shown it to be abundantly expressed in differentiated luminal alveolar cells (Li et al., 2003; Smith et al., 1990).

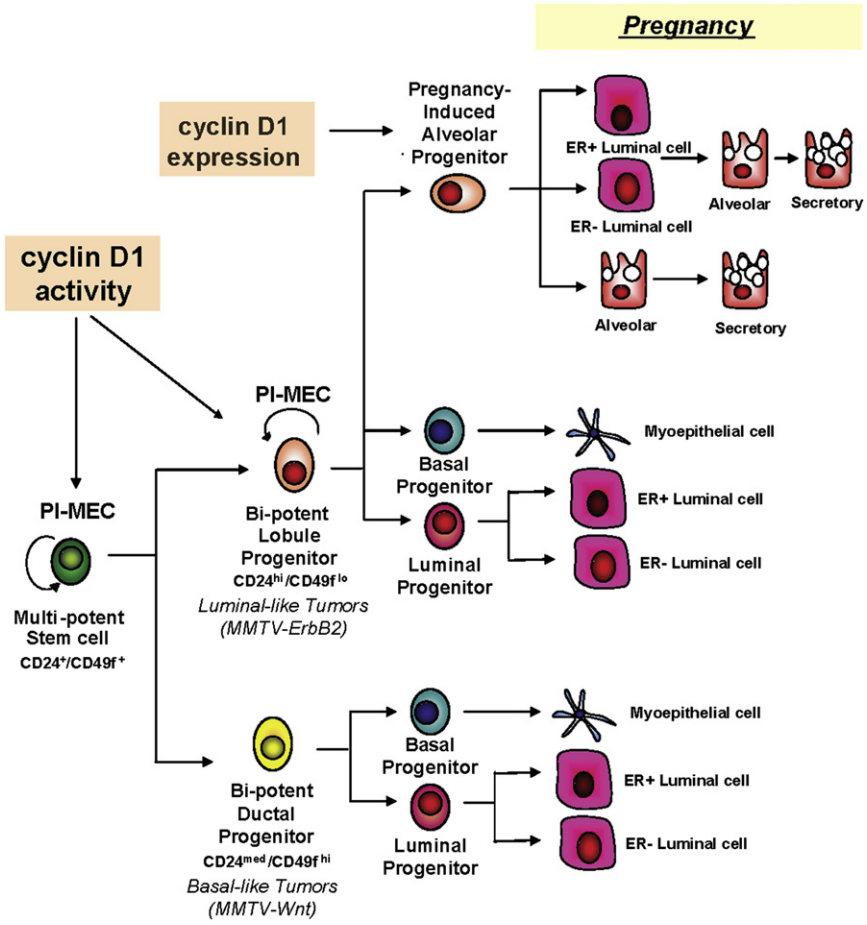

Figure 6. The Role of Cyclin D1 in the Mammary Epithelial Hierarchy

A proposed model of the mammary epithelial cell developmental hierarchy in which cyclin D1 expression and activity are required for the maintenance of the lobule progenitors, which are synonymous with the PI-MEC population.

We found no K6-positive cells in cyclin $D1^{KE/KE}$ mammary tissues (data not shown). However, not all luminal markers were misexpressed, given that the expression of estrogen (ERα) and progesterone receptors (PR-A and PR-B) was similar in luminal cells from both cyclin $D1^{KE/KE}$ and cyclin $D1^{+/+}$ glands (Figure 5A and data not shown). These data indicate that despite normal histological appearance, mammary ducts in cyclin $D1^{KE/KE}$ mice exhibit altered luminal cell differentiation.

Given these findings, we next examined ductal outgrowths from cyclin $D1^{+/+}$ and cyclin $D1^{KE/KE}$ transplants for evidence of perturbed luminal epithelial differentiation. Indeed, luminal cells of cyclin $D1^{KE/KE}$ ductal outgrowths did not express abundant E-cadherin and were negative for keratin-18 expression (Figure 5B). Furthermore, while K6 positive cells were found in the transplantation outgrowths derived from the cyclin $D1^{+/+}$ MECs, no K6 expression was detected in cyclin $D1^{KE/KE}$ outgrowths (Figure S4A). K6-positive cells in wild-type ducts were localized to the inner layer of the ductal epithelium, were negative for SMA, and coexpressed GATA-3, the luminal marker and transcription factor required for luminal differentiation (Asselin-Labat et al., 2007; Kouros-Mehr et al., 2006). However, ductal outgrowths from cyclin $D1^{+/+}$ and cyclin $D1^{KE/KE}$ MECs both displayed a prominent outer layer of SMA-positive myoepithelial cells, indicating that this lineage was not perturbed.

To further evaluate the defects in luminal cell differentiation, we analyzed dispersed single-cell suspensions from cyclin $D1^{+/+}$ and cyclin $D1^{KE/KE}$ mammary tissues sorted by FACS. Differential staining of mammary epithelial cells on the basis of CD24 expression can discriminate between different lineages of mammary epithelial cells (Sleeman et al., 2006; Sleeman et al., 2007). Myoepithelial and luminal epithelial cells are identified as $CD24^{Low}$ and $CD24^{Hi}$, respectively, while CD24-negative cells are considered to be nonepithelial cells. Using this approach, we found a significant increase in the percentage of $CD24^{Low}$ (CD24L) cells and a significant reduction in the percentage of $CD24^{Hi}$ (CD24H) cells in cyclin $D1^{KE/KE}$ MECs (Figure 5C, upper panels). To confirm that the disproportionate percentage of CD24L cells in cyclin $D1^{KE/KE}$ glands were myoepithelial cells, sorted $CD24^{Low}$ and $CD24^{Hi}$ cells were directly cytospun on glass slides and stained for SMA and E-cadherin. As expected, most of the CD24L cells stained positive for SMA and negative for E-cadherin, while the majority of CD24H cells were E-cadherin positive and SMA negative (Figure 5C, lower panels, and Figure S4B). Next, gene expression patterns of $CD24^{Hi}$ cells were examined using quantitative real-time polymerase chain reaction (RT-PCR). We found that $CD24^{Hi}$ luminal cells derived from cyclin $D1^{KE/KE}$ glands exhibit a reduction of *CK18*, *GATA-3*, and *CK6* expression compared with cyclin $D1^{+/+}$ cells, confirming that luminal cells exhibited altered differentiation in the absence of cyclin D1 kinase activity (Figure 5D). These findings imply that in the absence of cyclin D1-dependent kinase activity, differentiation of luminal cells is impaired and is accompanied by an accumulation of myoepithelial cells.

DISCUSSION

Our results, combined with those of others (Smith, 1996; Smith and Medina, 2008), support a more complex model of mammary gland hierarchy and differentiation. Multipotent $CD24^{+}CD49f^{+}$ stem cells (PI-MECs) give rise to lineage-committed lobule progenitor cells (also termed PI-MECs in parous mice) and ductal progenitor cells, both of which have the capacity to give rise to luminal and myoepithelial cells, but exhibit different functional outgrowth potential (Figure 6). We found that PI-MECs require cyclin D1 kinase activity for their self-renewal because ductal and lobule outgrowth potential were significantly impaired following transplantation into clear fat pads. In addition, in

mammary glands that could not maintain PI-MECs, luminal epithelial cell differentiation and tissue regeneration after serial rounds of pregnancy/lactation was also impaired. These data indicate that maintenance of PI-MECs and their progeny is necessary for long-term mammary tissue homeostasis and differentiation. Moreover, these data are consistent with previous reports, which have demonstrated that PI-MECs contain both multipotent stem cells that self-renew and generate diverse epithelial lineages of the murine mammary gland as well as lobule-committed progenitors (Boulanger et al., 2005; Henry et al., 2004; Smith and Medina, 2008; Wagner et al., 2002).

PI-MECs have also been reported to express both CD24 and CD49f surface markers (Boulanger et al., 2005; Henry et al., 2004; Smith and Medina, 2008; Wagner et al., 2002). Consistent with this notion, we observed that both $CD24^{Hi}CD49f^{Low}$ and $CD24^{Med}CD49f^{Hi}$ cells could regenerate complex mammary trees composed of ducts, lobules, and alveoli when transplanted into pregnant hosts. Remarkably, we found that while $CD24^{Hi}CD49f^{Low}$ cells produced complex mammary outgrowths when implanted into cleared fat pads of nulliparous hosts, $CD24^{Med}CD49f^{Hi}$ cells failed to develop ductal structures that contained side branches or lobules. This suggests that multipotent stem cells are a minority subpopulation within $CD24^{Med}CD49f^{Hi}$ cells that are only stimulated in the presence of pregnancy hormones. Therefore, it will be of great interest to identify additional markers beyond CD24 and CD49f that can further distinguish between multipotent stem cells and lineage-committed progenitor cells.

It is worth noting that our findings are not inconsistent with previous reports, but rather extend the mammary hierarchy to incorporate the different functional lineages and anatomical structures that make up breast tissue. It is also worth noting that the transplant experiments described in this study were conducted in the presence of Matrigel. We did find that in vivo reconstitution activity of sorted $CD24^{Hi}CD49f^{Low}$ cells was greatly compromised in the absence of Matrigel (data not shown). Consistent with this notion, coinjection with Matrigel in other stem cell assays has been reported to enhance engraftment of primary epithelial cells (Quintana et al., 2008). Consequently, the observations we have reported herein provide strong evidence that modification of the transplantation assay can enable the detection of progenitor cell activity and regeneration potential of mouse mammary epithelial cells. This has provided for a means to identify additional stem/progenitor cell populations that appear to have diverse functional activities and exhibit unique sensitivity to pregnancy hormones.

In addition to expanding the mammary gland hierarchy, our data demonstrate that: (1) cyclin D1 activity is required for the maintenance of PI-MECs and lobule progenitor cells; (2) PI-MECs are the target of *MMTV-ErbB2*-mediated tumorigenesis; and (3) the inability to maintain PI-MECs and lobule progenitor cells results in mammary tissues with a disproportionate number of myoepithelial cells and impaired state of differentiation of luminal epithelial cells.

Our data can also explain the described differential susceptibility of cyclin D1 knockout mice to different mammary oncogenes (Yu et al., 2001). Accordingly, *MMTV-Wnt1*- and *MMTV-Myc*-driven tumors are likely to arise from ductal progenitor cells, whereas *MMTV-Ras* and *MMTV-ErbB2* tumors arise from lobule progenitor cells (Chepko et al., 2005; Shackleton et al., 2006). Recently, $CD29^{Hi}CD24^{Med}$ cells were found to expand in early hyperplastic lesions of *MMTV-Wnt1* mammary glands but not in those transformed by *MMTV-ErbB2* (Shackleton et al., 2006). It was proposed that this population of progenitor cells is likely to be the cellular origin of MMTV-Wnt1-driven transformation but not that of *MMTV-ErbB2*. As shown in our model (Figure 6), cyclin D1 kinase activity is required for the maintenance of lobule progenitors, the tumor-initiating cells of *MMTV-ErbB2*- and *MMTV-Ras*-mediated tumorigenesis, but is not required for the maintenance of the ductal progenitors, the tumor-initiating cells of *MMTV-Wnt1* and *MMTV-Myc*. In fact, we saw an increase in the $CD24^{Med}CD49f^{Hi}$ population that contains ductal progenitors in mammary glands lacking cyclin D1 activity, suggesting that loss of cyclin D1 could actually increase *Wnt1*- or *Myc*-induced tumorigenesis. In support of this possibility, cyclin D1 knockout mice that constitutively express beta-catenin in the mammary gland have an increased frequency and decreased latency for tumor development compared with *MMTV-Wnt1* tumorigenesis (Rowlands et al., 2003).

Our initial finding that during a first pregnancy the cyclin $D1^{KE/KE}$ MECs are able to expand their lobuloalveolar units similar to those of cyclin $D1^{+/+}$ MECs made it difficult to dissect the role of cyclin D1 as a regulator of development from that important for transformation. However, after successive pregnancies we observed a significant reduction in lobuloalveoli development similar to, but not as profound as, the reduction seen the cyclin D1 knockout mouse after a first pregnancy. This delay in the developmental phenotype relative to that seen in the cyclin D1 knockout animals may indicate that a noncatalytic function of cyclin D1/Cdk complexes, such as titration of the cell-cycle inhibitors $p27^{Kip1}$ and $p21^{Cip1}$, may be sufficient for the expansion of the ductal progenitors but only weakly able to influence lobule progenitor cell proliferation. The identity of the critical targets of these catalytic and noncatalytic functions of cyclin D1 in the mammary epithelium remains to be determined.

Although not as well studied, there is evidence to support the existence of a mammary epithelial hierarchy with bipotent progenitors in the human breast (Stingl et al., 2001). Recently a unique population of cells that could be the human lobule progenitor has been identified. These cells are $EpCam^{Hi}CD49f^{+}$ (resembling the $CD24^{Hi}CD49f^{+}$ population in mice), exhibit increased colony-forming ability, and can give rise to both luminal and myoepithelial cells (Villadsen et al., 2007). Studying the effects of loss of cyclin D1 or CDK4 on this population could potentially help us to understand the role of cyclin D1 in the human breast as well as further delineate the human mammary epithelial hierarchy.

Lastly, this study reiterates the importance of tailoring the treatment in breast cancer as well as other cancers to the biology of the tumor. As we show here, cyclin D1-associated kinase activity is critical for the maintenance of the cells driving *MMTV-ErbB2* tumors as well as other luminal tumors, but not for the cells driving tumors originating from ductal progenitor cells. Our studies support the notion that treatments targeting cyclin D1 will be effective for the prevention and treatment of luminal type cancers but will most likely not be effective, and may even be deleterious, in patients with basal-type cancers.

EXPERIMENTAL PROCEDURES

Mouse Strains

The generation of cyclin D1$^{KE/KE}$ mice was described previously (Landis et al., 2006). The *MMTV–ErbB2* mouse (strain TG.NK) used in this study has been described elsewhere (Muller et al., 1988). *ROSA26-GFP* mice were purchased from the Jackson Laboratories. *WAP-cre* transgenic mice were obtained from the NCI Mouse Models of Human Cancers Consortium. All animals used were treated humanely and in accordance with protocols approved by the Institutional Animal Care and Use Committee at Tufts Medical Center.

Preparation of Single-Cell Suspensions

Mammary glands were harvested from 12-week-old mice (except for PI-MECs studies in which mice were sacrificed 6 weeks postinvolution). Glands were mechanically disaggregated and then digested with collagenase (Sigma) and Hyaluronidase (Sigma) for 3–6 hr at 37°C. The resultant organoids were further digested in 0.25% trypsin-EDTA (2 min) and Dispase/DNaseI (5 min), and then filtered through a 40 μm mesh. When necessary, Lin+ cells (CD45$^+$, CD31$^+$, and Ter 119$^+$) were immunomagnetically removed from freshly isolated cells using the Easysep mouse mammary stem cell enrichment kit (Stem Cell Technologies).

Mammary Fat-Pad Transplants

For limiting dilution experiments, freshly isolated MECs were resuspended in 40 μl phosphate-buffered saline (PBS) and injected into cleared inguinal fat pads of 3-week-old nonobese diabetic/severe combined immunodeficient mice (Deome et al., 1959). Cyclin D1$^{KE/KE}$ or cyclin D1$^{+/+}$ MECs were transplanted into contralateral inguinal fat pads. Five weeks after transplantation glands were harvested and processed for whole mounting. Freshly sorted CD24^{Hi}CD49f^{Low} and CD24^{Med}CD49f^{Hi} cells purified from Balb/c mammary glands were resuspended in 25 μl Matrigel:Medium (1:3) solution and injected into cleared inguinal fat pads of syngeneic Balb/c female mice. For nulliparous studies, 3-week-old Balb/c females were used as hosts. For pregnant hosts, 3-week-old Balb/c female mice were cleared of their endogenous epithelium and allowed to mature for 5 weeks. At 8 weeks, mice were mated and examined daily for positive plugs. Mice that were negative for plugs were used as age-matched nulliparous controls. Pregnant and nonpregnant control hosts were injected with sorted cells, and 3 weeks after transplantation glands were harvested and processed for whole mounting. Before being sacrificed, the stage at the estrous cycle of each recipient mouse was determined by microscopic inspection of hematoxylin-stained vaginal smears. Transplantations were considered negative if there were no epithelial outgrowths, and positive if the outgrowth appeared to originate from a central location and branch out in multiple directions. If the outgrowth appeared to originate from the side of the gland and the branching was mainly unidirectional, the transplant was considered as a failed clearance. Percent filling was quantified under a dissecting microscope at 2X magnification using the following formula: % filling = length of ductal outgrowth/ total length of mammary fat pad.

Whole Mounts

Mammary glands were spread onto glass slides and fixed in glacial acetic acid:ethanol (1:3), hydrated, and stained overnight in 0.2% carmine red. Glands were subsequently dehydrated with graded ethanol solutions, cleared in toluene and mounted.

Immunostaining

Tissue sections were incubated overnight at 4°C with primary antibodies diluted in 2% bovine serum albumin PBS. Secondary antibodies were applied for 1 hr at room temperature. Sections were counterstained with DAPI whenever necessary. For cells cytospun directly onto glass slides, fixation was carried out in methanol:acetone (1:1) at −20°C for 10 min. A Nikon Eclipse 80t microscope and SPOT camera were used for analyzing and photographing the stained sections. The antibodies used included SMA (Neomarkers), E-cadherin (Santa Cruz biotechnologies), CK18 (Abcam), K6 (Covance), GATA-3 (Santa Cruz Biotechnologies), and ERα (Dako).

Flow Cytometry

Freshly isolated Lin(−) cells (CD45$^-$, CD31$^-$, and Ter119$^-$) were incubated with primary antibodies according to the manufacturer's instructions (Stem Cell Technology). Antibodies used were CD29 (Chemicon), CD24 and CD49f (Stem Cell Technology), CD45 (Caltag), and SCA-1 (BD PharMingen). Cell sorting was carried out with a modular flow cytometer (Beckman-Coulter) and analysis was done with FlowJo.

In Vitro Assays

Freshly isolated MECs (5 × 10^4) were seeded on 10 cm plates containing subconfluent, gamma-irradiated NIH 3T3 cells (5 Gy) as feeder layers. On day 5, mammary colonies were fixed with methanol, stained with crystal violet, and counted. For sphere-formation assays, freshly isolated MECs (20,000 cells per 3 ml) were plated on nonadherent plates (Corning) in serum-free medium. Primary spheres were dissociated with trypsin after 3 weeks and filtered through a 40 μM mesh. Single cells were plated again in nonadherent plates for secondary spheres formation. When necessary, secondary spheres were also dissociated and single cells embedded in Matrigel (BD Biosciences) as described elsewhere (Debnath et al., 2003). The resultant acini were fixed with 2% PFA on day 7 and stained as described previously (Debnath et al., 2003). Images were captured with a Leica TCS SP2 confocal microscope.

Quantitative RT-PCR

Total RNA from sorted cells was extracted with the RNeasy Mini Kit (QIAGEN). cDNA was prepared with an iScript kit (Bio-Rad) and PCR was carried out with SYBR Green (QIAGEN). The following primers were used in this study: *CK18* forward 5′-CTTGCTGGAGGATGGAGAAG-3′ and CK18 reverse 5′-CTGG CTGGAGCAGGAGATTCG-3′; *GATA-3* forward 5′-AGCCACATCTCTCCCTT CAG-3′ and *GATA-3* reverse 5′-AGGGCTCTGCCTCTCTAACC-3′; *CK6* forward 5′-AGAGAGGGGTCGCATGAACT-3′ and CK6 reverse 5′-TCATCTGT TAGACTGTCTGCCTT-3′; *CD61* forward 5′-CCACACGAGGGGTGAACT-3′ and CD61 reverse 5′-CTTCAGGTTACATGGGGGTGA-3′. Samples were run on an Opticon2 detection system (MJ research). *GAPDH* was used as an internal control. Analysis was performed with the delta-delta ct method with the comparator being RNA extracted from wild-type unsorted cells.

Statistical Analysis

p values were determined with a two-tailed distribution and two-sample unequal variance Student's t test.

SUPPLEMENTAL INFORMATION

Supplemental Information includes four figures and one table and can be found with this article online at doi:10.1016/j.ccr.2009.11.024.

ACKNOWLEDGMENTS

The authors thank the members of the Hinds and Kuperwasser labs for their helpful comments. This work was supported by NIH grant CA096527 (P.W.H.), by grants from the National Center for Research Resources K01-RR021858 (L.A.), and by the Breast Cancer Research Foundation (C.K.). C.K. is a Raymond and Beverly Sackler Foundation Scholar. R.J. was supported by training grant T32 CA009429.

Received: July 17, 2008
Revised: June 25, 2009
Accepted: November 30, 2009
Published: January 19, 2010

REFERENCES

Asselin-Labat, M.L., Sutherland, K.D., Barker, H., Thomas, R., Shackleton, M., Forrest, N.C., Hartley, L., Robb, L., Grosveld, F.G., van der Wees, J., et al. (2007). Gata-3 is an essential regulator of mammary-gland morphogenesis and luminal-cell differentiation. Nat. Cell Biol. *9*, 201–209.

Baker, G.L., Landis, M.W., and Hinds, P.W. (2005). Multiple functions of D-type cyclins can antagonize pRb-mediated suppression of proliferation. Cell Cycle *4*, 330–338.

Booth, B.W., Boulanger, C.A., and Smith, G.H. (2007). Alveolar progenitor cells develop in mouse mammary glands independent of pregnancy and lactation. J. Cell. Physiol. *212*, 729–736.

Boulanger, C.A., Wagner, K.U., and Smith, G.H. (2005). Parity-induced mouse mammary epithelial cells are pluripotent, self-renewing and sensitive to TGF-beta1 expression. Oncogene *24*, 552–560.

Chepko, G., Slack, R., Carbott, D., Khan, S., Steadman, L., and Dickson, R.B. (2005). Differential alteration of stem and other cell populations in ducts and lobules of TGFalpha and c-Myc transgenic mouse mammary epithelium. Tissue Cell *37*, 393–412.

Debnath, J., Muthuswamy, S.K., and Brugge, J.S. (2003). Morphogenesis and oncogenesis of MCF-10A mammary epithelial acini grown in three-dimensional basement membrane cultures. Methods *30*, 256–268.

Deome, K.B., Faulkin, L.J., Jr., Bern, H.A., and Blair, P.B. (1959). Development of mammary tumors from hyperplastic alveolar nodules transplanted into gland-free mammary fat pads of female C3H mice. Cancer Res. *19*, 515–520.

DiMeo, T.A., Anderson, K., Phadke, P., Fan, C., Perou, C.M., Naber, S., and Kuperwasser, C. (2009). A novel lung metastasis signature links Wnt signaling with cancer cell self-renewal and epithelial-mesenchymal transition in basal-like breast cancer. Cancer Res. *69*, 5364–5373.

Dontu, G., Abdallah, W.M., Foley, J.M., Jackson, K.W., Clarke, M.F., Kawamura, M.J., and Wicha, M.S. (2003). In vitro propagation and transcriptional profiling of human mammary stem/progenitor cells. Genes Dev. *17*, 1253–1270.

Fantl, V., Stamp, G., Andrews, A., Rosewell, I., and Dickson, C. (1995). Mice lacking cyclin D1 are small and show defects in eye and mammary gland development. Genes Dev. *9*, 2364–2372.

Gauthier, M.L., Berman, H.K., Miller, C., Kozakeiwicz, K., Chew, K., Moore, D., Rabban, J., Chen, Y.Y., Kerlikowske, K., and Tlsty, T.D. (2007). Abrogated response to cellular stress identifies DCIS associated with subsequent tumor events and defines basal-like breast tumors. Cancer Cell *12*, 479–491.

Henry, M.D., Triplett, A.A., Oh, K.B., Smith, G.H., and Wagner, K.U. (2004). Parity-induced mammary epithelial cells facilitate tumorigenesis in MMTV-neu transgenic mice. Oncogene *23*, 6980–6985.

Herschkowitz, J.I., Simin, K., Weigman, V.J., Mikaelian, I., Usary, J., Hu, Z., Rasmussen, K.E., Jones, L.P., Assefnia, S., Chandrasekharan, S., et al. (2007). Identification of conserved gene expression features between murine mammary carcinoma models and human breast tumors. Genome Biol. *8*, R76.

Hinds, P.W., Dowdy, S.F., Eaton, E.N., Arnold, A., and Weinberg, R.A. (1994). Function of a human cyclin gene as an oncogene. Proc. Natl. Acad. Sci. USA *91*, 709–713.

Kordon, E.C., and Smith, G.H. (1998). An entire functional mammary gland may comprise the progeny from a single cell. Development *125*, 1921–1930.

Kouros-Mehr, H., Slorach, E.M., Sternlicht, M.D., and Werb, Z. (2006). GATA-3 maintains the differentiation of the luminal cell fate in the mammary gland. Cell *127*, 1041–1055.

Landis, M.W., Pawlyk, B.S., Li, T., Sicinski, P., and Hinds, P.W. (2006). Cyclin D1-dependent kinase activity in murine development and mammary tumorigenesis. Cancer Cell *9*, 13–22.

Li, Y., Welm, B., Podsypanina, K., Huang, S., Chamorro, M., Zhang, X., Rowlands, T., Egeblad, M., Cowin, P., Werb, Z., et al. (2003). Evidence that transgenes encoding components of the Wnt signaling pathway preferentially induce mammary cancers from progenitor cells. Proc. Natl. Acad. Sci. USA *100*, 15853–15858.

Li, Z., Tognon, C.E., Godinho, F.J., Yasaitis, L., Hock, H., Herschkowitz, J.I., Lannon, C.L., Cho, E., Kim, S.J., Bronson, R.T., et al. (2007). ETV6-NTRK3 fusion oncogene initiates breast cancer from committed mammary progenitors via activation of AP1 complex. Cancer Cell *12*, 542–558.

Liu, J.C., Deng, T., Lehal, R.S., Kim, J., and Zacksenhaus, E. (2007). Identification of Tumorsphere- and Tumor-Initiating Cells in HER2/Neu-Induced Mammary Tumors. Cancer Res. *67*, 8671–8681.

Matulka, L.A., Triplett, A.A., and Wagner, K.U. (2007). Parity-induced mammary epithelial cells are multipotent and express cell surface markers associated with stem cells. Dev. Biol. *303*, 29–44.

Muller, W.J., Sinn, E., Pattengale, P.K., Wallace, R., and Leder, P. (1988). Single-step induction of mammary adenocarcinoma in transgenic mice bearing the activated c-neu oncogene. Cell *54*, 105–115.

Perou, C.M., Sorlie, T., Eisen, M.B., van de Rijn, M., Jeffrey, S.S., Rees, C.A., Pollack, J.R., Ross, D.T., Johnsen, H., Akslen, L.A., et al. (2000). Molecular portraits of human breast tumours. Nature *406*, 747–752.

Quintana, E., Shackleton, M., Sabel, M.S., Fullen, D.R., Johnson, T.M., and Morrison, S.J. (2008). Efficient tumour formation by single human melanoma cells. Nature *456*, 593–598.

Rowlands, T.M., Pechenkina, I.V., Hatsell, S.J., Pestell, R.G., and Cowin, P. (2003). Dissecting the roles of beta-catenin and cyclin D1 during mammary development and neoplasia. Proc. Natl. Acad. Sci. USA *100*, 11400–11405.

Shackleton, M., Vaillant, F., Simpson, K.J., Stingl, J., Smyth, G.K., Asselin-Labat, M.L., Wu, L., Lindeman, G.J., and Visvader, J.E. (2006). Generation of a functional mammary gland from a single stem cell. Nature *439*, 84–88.

Sicinski, P., Donaher, J.L., Parker, S.B., Li, T., Fazeli, A., Gardner, H., Haslam, S.Z., Bronson, R.T., Elledge, S.J., and Weinberg, R.A. (1995). Cyclin D1 provides a link between development and oncogenesis in the retina and breast. Cell *82*, 621–630.

Sleeman, K.E., Kendrick, H., Ashworth, A., Isacke, C.M., and Smalley, M.J. (2006). CD24 staining of mouse mammary gland cells defines luminal epithelial, myoepithelial/basal and non-epithelial cells. Breast Cancer Res. *8*, R7.

Sleeman, K.E., Kendrick, H., Robertson, D., Isacke, C.M., Ashworth, A., and Smalley, M.J. (2007). Dissociation of estrogen receptor expression and in vivo stem cell activity in the mammary gland. J. Cell Biol. *176*, 19–26.

Smith, G.H. (1996). Experimental mammary epithelial morphogenesis in an in vivo model: Evidence for distinct cellular progenitors of the ductal and lobular phenotype. Breast Cancer Res. Treat. *39*, 21–31.

Smith, G.H., and Medina, D. (2008). Re-evaluation of mammary stem cell biology based on in vivo transplantation. Breast Cancer Res. *10*, 203.

Smith, G.H., Mehrel, T., and Roop, D.R. (1990). Differential keratin gene expression in developing, differentiating, preneoplastic, and neoplastic mouse mammary epithelium. Cell Growth Differ. *1*, 161–170.

Stingl, J., Eaves, C.J., Zandieh, I., and Emerman, J.T. (2001). Characterization of bipotent mammary epithelial progenitor cells in normal adult human breast tissue. Breast Cancer Res. Treat. *67*, 93–109.

Stingl, J., Eirew, P., Ricketson, I., Shackleton, M., Vaillant, F., Choi, D., Li, H.I., and Eaves, C.J. (2006). Purification and unique properties of mammary epithelial stem cells. Nature *439*, 993–997.

Villadsen, R., Fridriksdottir, A.J., Ronnov-Jessen, L., Gudjonsson, T., Rank, F., LaBarge, M.A., Bissell, M.J., and Petersen, O.W. (2007). Evidence for a stem cell hierarchy in the adult human breast. J. Cell Biol. *177*, 87–101.

Wagner, K.U., Boulanger, C.A., Henry, M.D., Sgagias, M., Hennighausen, L., and Smith, G.H. (2002). An adjunct mammary epithelial cell population in parous females: Its role in functional adaptation and tissue renewal. Development *129*, 1377–1386.

Yu, Q., Geng, Y., and Sicinski, P. (2001). Specific protection against breast cancers by cyclin D1 ablation. Nature *411*, 1017–1021.